

ZEISS Lightsheet 7

How to Get Best Images with Various Types of
Immersion Media and Clearing Agents



Seeing beyond

ZEISS Lightsheet 7

How to Get Best Images with Various Types of Immersion Media and Clearing Agents

Authors: Dr. Harald Schadwinkel, Dr. Olaf Selchow,
Dr. Klaus Weisshart, Dr. Jakob Haarstrich,
Jan Birkenbeil
Carl Zeiss Microscopy GmbH, Germany

Date: March 2020

In recent years, light sheet fluorescence microscopy (LSFM) with its unique illumination principle has become a standard method to image large optically cleared specimens in toto, and with subcellular resolution. ZEISS Lightsheet 7 can be equipped with dedicated optics, sample chambers and sample holders to accurately adjust to the refractive index of all common clearing methods and immersion media to allow imaging of large samples, even whole mouse brains. In the following, we will explain how changes in refractive index (RI) in the sample space influence the optics of the imaging system and how understanding the optical principles and choosing appropriate components and imaging settings will help to improve the image quality substantially.

Basic Optics

ZEISS Lightsheet 7 uses the basic optical principle of light sheet microscopes with illumination objectives that form the sheet of light (green in Figure 1) and a detection objective that collects the fluorescence signal in a perpendicular direction (red in Figure 1). The sample chamber (blue) in the Figure is filled with an imaging medium specific for the required experimental conditions. For example, imaging of living specimens is typically conducted in aqueous media with a RI around $n_0 \sim 1.33$ (left sketch in Figure 1). The illumination lenses are aligned to focus on the center of the detection field of view, i.e., the optical axis of the detection objective.

If the sample chamber is now filled with a medium of higher refractive index – which is typical for most clearing applications – the focus position of both

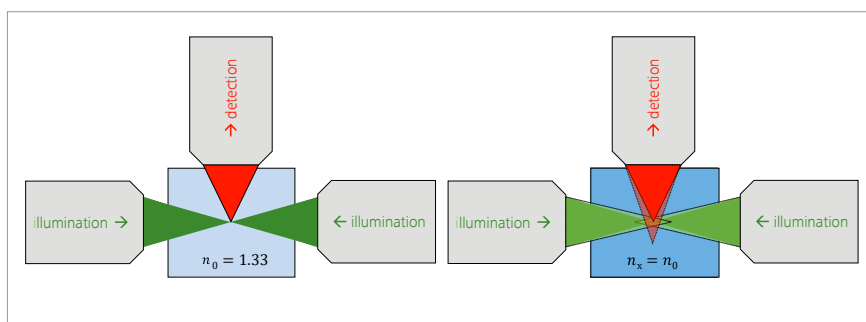


Figure 1 Focus shift due to refractive index variations. Left: water immersion, right: chamber filled with a medium of higher RI.

illumination and detection lenses will shift further away from the objective. In the sketch on the right in Figure 1 we assume a higher refractive index $n_x > n_0$.

This focus shift is roughly proportional to both the nominal distance L_0 the light travels inside the medium¹ and the ratio of the two refractive indices:

$$L_x - L_0 \cong L_0 \left(\frac{n_x}{n_0} - 1 \right)$$

Recent development of new methods for optical clearing of tissue made imaging of larger specimens, e.g. tissue sections, spheroids, organoids, organs or even whole model organisms increasingly important^{2,3,4,5}. The refractive indices of the respective imaging media are well above the RI of water⁶. Both these factors increase focal shifts and their effects multiply.

ZEISS Lightsheet 7 offers two opposing illumination objectives and both focal planes coincide in the chamber's center by design, producing the thinnest light sheet (beam waist) on the axis of the detection objective. If the medium inside the chamber deviates in refractive index from what the chamber and lenses are designed for, the focal shifts for the two opposing illumination objectives will result in an increased thickness ($2r_0$) of the illumination light sheet.⁷

$$r_x \cong L_0 \cdot NA \cdot \left(\frac{1}{n_x} - \frac{1}{n_0} \right)$$

This effect will directly reduce the ability of the system to produce thin optical sections and therefore increase the level of out of focus signal and, as a consequence, reduce axial resolution.

We illustrate this effect with some numbers: Say, the sample chamber is approximately $2L_0=30$ mm wide. If a sample chamber that is aligned for use with FocusClear™ ($n_0=1.45$) is now filled with RapiClear 1.52® ($n_x=1.52$), the waist would shift from $L_0=15$ mm to $L_x \approx 15.7$ mm. The thickness of the illumination light sheet from an illumination lens with $NA=0.2$ would increase from $2r_0 \approx 1.7$ μm to $2r_x \approx 100$ μm.

In classic LSFM systems, both focal shift and increased thickness are compensated by adapting the width of the sample chamber to different media and their refractive indices. This approach is conceptually simple, but it requires a dedicated sample chamber with appropriate width for each refractive index.

The multitude of new immersion media and emerging clearing protocols limits the practicality of this approach.

Detection Objective Magnification	FOV [μm]	Maximum range for n_x
5x	1742	1.408 ... 1.492
10x	873	1.429 ... 1.471
20x	437	1.439 ... 1.461
40x	218	1.445 ... 1.455
63x	139	1.447 ... 1.453

Table 1

While the increase in light sheet thickness seems more dramatic than the illumination focus shift⁸, for high magnification objectives, the focal shift can become so large, that the illumination focus – the light sheet waist – lies completely outside of the field of view (FOV) of the detection objective. The equation below describes the range of accessible refractive indices for which the focal shift is to be smaller than $FOV/2$. This would imply a light sheet waist at the edge of the field of view. We use this condition here to get an overview of the extreme cases. In a practical situation, one would certainly need even smaller focus shifts than that.

$$L_x - L_0 = L_0 \left(\frac{n_{max}}{n_0} - 1 \right) < \frac{FOV}{2}$$

Let's have a closer look at what this really means for imaging. The following table shows how small the tolerable deviation from the ideal refractive index should be, before the illumination beam waist is shifted outside of the FOV. (in this theoretical example, we use illumination $NA=0.2$, $2L_0=30$ mm and a sample chamber designed for FocusClear™, $n_0=1.45$, and assume zoom setting = 1x and a pco.edge 4.2 CLHS sensor).

The popular use of zoom optics in the detection light path sets an even tighter limit to the tolerable range of refractive indices. Table 1 clearly shows that focus-adjustable optics are the best solution for proper alignment of the light sheet waist to the center of the FOV (Figure 2).

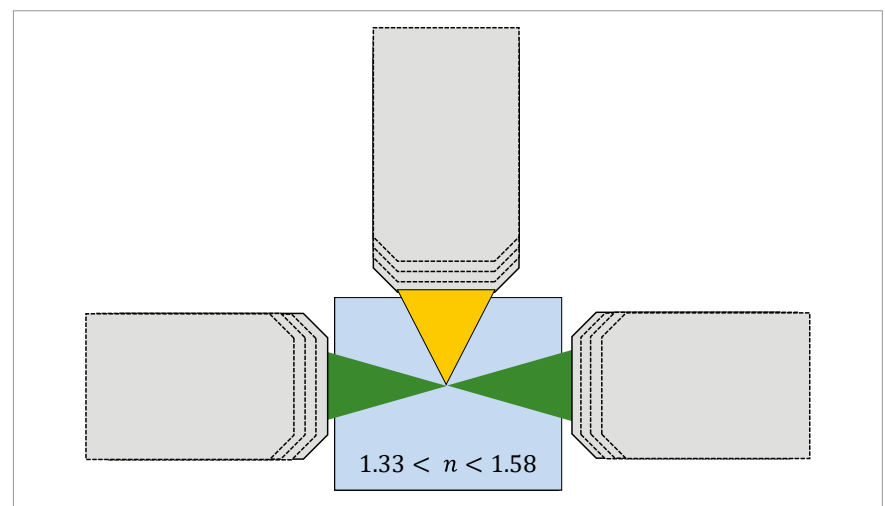


Figure 2 Compensating focal shift for a wide range of refractive indices (1.33 to 1.58) by focusing the objectives.



Figure 3 ZEISS Lightsheet 7 illumination objective 10x/0.2 f.c. and detection optics 5x/0.16 f.c. Both feature a new focus adjustment ring to tune the illumination (light sheet) and detection focus to the chosen medium.

That's why the new illumination and detection objective lenses for ZEISS Lightsheet 7 now allow to precisely adjust the illumination light sheet and the detection focus to a wide range of water based and organic clearing agents with refractive indices from 1.33 to 1.58. This new focusing mechanism is implemented in all illumination objectives and the 5x detection objective for clearing and permits to perfectly match the various RIs of different imaging media with one single sample chamber design (Figure 3).

Refractive index mismatch and resulting optical aberrations

Optical aberrations are image imperfections that occur due to a refractive index mismatch, even after correcting the focal shift as described above. For a comprehensive description of

optical aberrations, we recommend having a look at the literature¹⁰. In this Technical Note, we will only discuss the most relevant optical aberrations, *i.e.*, *spherical aberration* and *longitudinal chromatic aberration*.

Spherical aberration

Spherical aberration occurs, when not all rays that contribute to a focused cone of light will meet in the cone's tip. Figure 4 (left) shows a focused cone of light. On the right side, an enlarged and perpendicular view of the focal plane is shown.

The rays on and close to the optical axis (z-axis) converge in a shifted focus at L_x (shown as red dot on the perpendicular view on the right of Figure 4). The rays from the outer part of the cone converge in a slightly different focus and lie on the green circle of the perpendicular section on the right of Figure 4. This spherical aberration is usually much smaller than the focal shift and, for illustration purposes, the right side of Figure 4 shows a significantly enlarged view with respect to the sketch on the left side of Figure 4. With ZEISS optics for Lightsheet 7, spherical aberrations are negligible when using the imaging medium, the optics have been designed for. Remaining aberrations only occur due to a refractive index mismatch.

Spherical aberrations depend on the angle of rays that converge in a focus, the outer (green) rays of the cone are defined by the numerical aperture (NA) of the focusing optics. The formula

$$L'_x = L_0 \cdot \frac{\tan(\arcsin(\frac{NA}{n_0}))}{\tan(\arcsin(\frac{NA}{n_x}))}$$

describes the focal shift in a generalized form and includes the ray angle in the numerical aperture ($NA = n_{\sin \alpha}$). On axis or

for small angles ($NA \Rightarrow 0$ and $L'_x \Rightarrow L_x$) it reduces to the simpler form given in Figure 4. This focal shift with ray angle is called longitudinal spherical aberration (LSA) and represents the shift along the optical axis (z-axis). The larger this shift or the LSA, the larger the green circle in the right section of Figure 4. This circle extends in the plane orthogonal to the optical axis and is called transverse spherical aberration. Thus, transverse and longitudinal

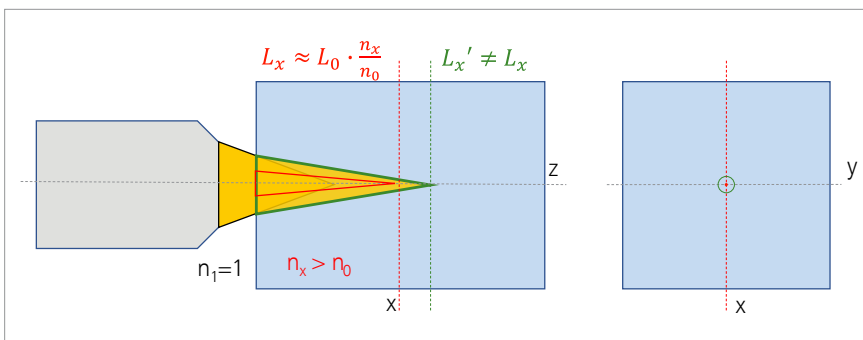


Figure 4 Spherical aberration, when not all rays of a focused cone of light converge in a common focus point. The axial rays meet in the red focus point, whereas the rays at the edge of the cone have a different focus point.

spherical aberrations are two sides of the same optical effect. Spherical aberration degrades image quality with blur.

In practice, the LSA is smaller than the primary focal shift described in the previous section.

In summary, the primary refractive index-dependent focal shift is angle-independent and occurs also for small angles (hence small NA, 5×/0.16). The longitudinal spherical aberration increases with higher NA and can become the dominant effect (e.g., with 20×/1.0 objective lenses).

To get best image quality, ZEISS Light-sheet 7 optics allow to correct the focal shift with the illumination optics (NA=0.1 and NA=0.2) as well as for the low magnification (5×) detection objective (NA=0.16).

Since spherical aberration mostly affects imaging with higher NA detection objectives (e.g. the 20×/1.0 clearing objectives), these objectives have therefore been designed to correct for spherical aberrations with a correction collar and allow compensation of refractive index



Figure 6 New Clr Plan-NEOFLUAR 20×/1.0 nd=1.53 with large correction range.

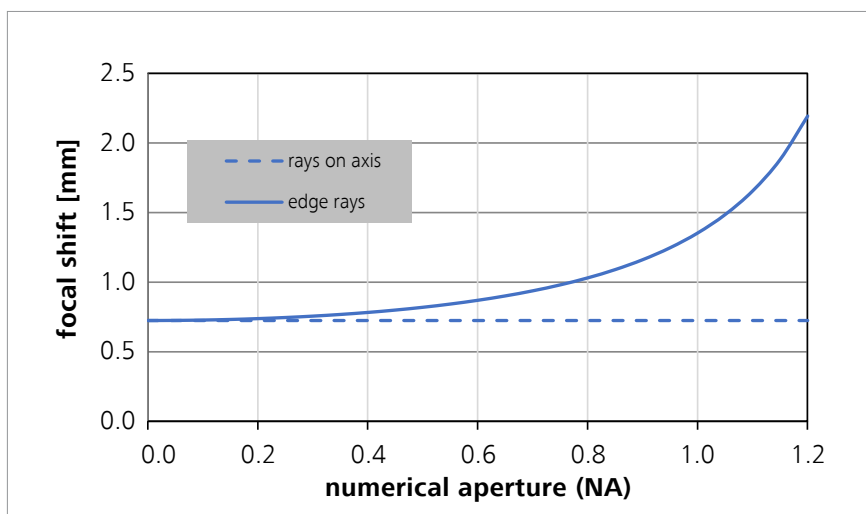


Figure 5 Focal shift for on-axis rays and edge rays inside a chamber $L_0=15$ mm that was designed for $n_0=1.45$ (e.g. Focus Clear® and is used with $n_x=1.52$ (e. g. Rapi Clear 1.52®).

mismatches of $\Delta n = \pm 0.03$ (Clr Plan-Apochromat 20× / 1.0 Corr nd=1.38 and Clr Plan-NEOFLUAR 20× / 1.0 Corr nd=1.45) or even $\Delta n = \pm 0.05$ for the new Clr Plan-NEOFLUAR 20×/1.0 Corr $n_d=1.53$.

Longitudinal chromatic aberration

Longitudinal chromatic aberration is easy to understand when considering that the refractive index depends on the

wavelength. Speaking about ‘the’ refractive index is therefore a simplification and ‘the’ refractive index usually refers to a reference wavelength in the visible spectral range – usually 546.1 nm (Mercury e-line) or 587.6 nm (Helium d-line). The figure below shows a selection of common imaging media and clearing agents and how their refractive indices vary with wavelength.

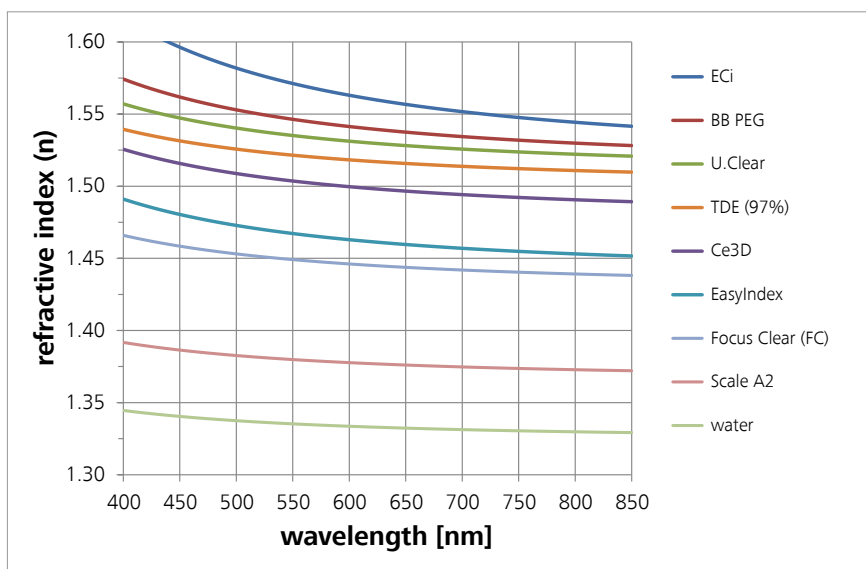


Figure 7 Refractive indices for various common imaging media. The broad range of main refractive indices as well as the range of dispersions are clearly visible.

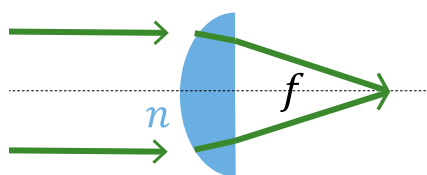
The variation or slope of the refractive index curve with wavelength is called dispersion. It is different for each medium. A common, still simplified, description for the dispersion is given by the Abbe number (defined by the relation of the refractive index at the Mercury e-line (546.1 nm) to the refractive index variation of the wavelength range from 488 nm to 640 nm):

$$v_{546} = \frac{n_{546} - 1}{n_{488} - n_{640}}$$

Both the main refractive indices and the dispersion of common imaging media vary significantly over the range of the visible spectrum:

$$1.33 < n < 1.57 \quad 19 < v < 56$$

If the refractive indices are known for the wavelengths used in the microscope, the analysis is simple and comes down to applying the formula for the focal shift with the appropriate refractive index $n(\lambda)$.



for which the focal length is given by the lens maker's formula:

$$\frac{1}{f} = (n_{lens} - 1) \cdot \left(\frac{1}{R_1} - \frac{1}{R_2} \right)$$

The radii of curvature R_1 and R_2 stay fixed, hence it is obvious that a change of refractive index $n(\lambda)$ with wavelengths will inevitably result in a variation of the focal length.

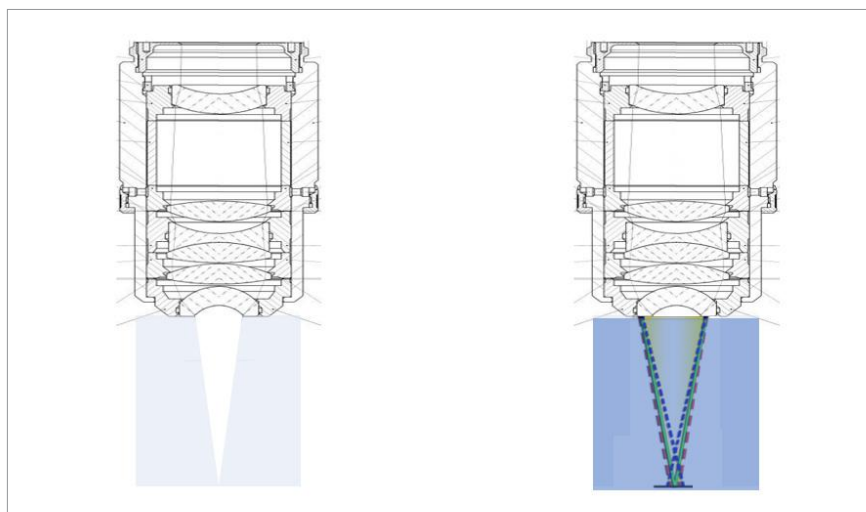


Figure 8 Left: A microscope objective designed to be used with a specific imaging medium, the rays for all wavelengths come to a common focus. Right: If the imaging medium is exchanged for one with a significantly different $n(\lambda)$, a wavelength dependent focus shift will occur.

To get a more realistic example, the single lens from the example above is substituted by a complex microscope objective with imaging medium in front.

By carefully combining lens shapes and materials in the objective, optical engineers can compensate for the variation of the refractive index $n(\lambda)$ of the imaging medium over a broad range of wavelengths λ . If the imaging medium

now changes, this compensation does not work and a focal shift between color channels will be visible. This focal shift is wavelength dependent.

Knowledge of refractive indices and dispersions of typical imaging media in the design process of objective lenses allows to minimize chromatic aberrations for a multitude of imaging media, as shown in Figure 9.

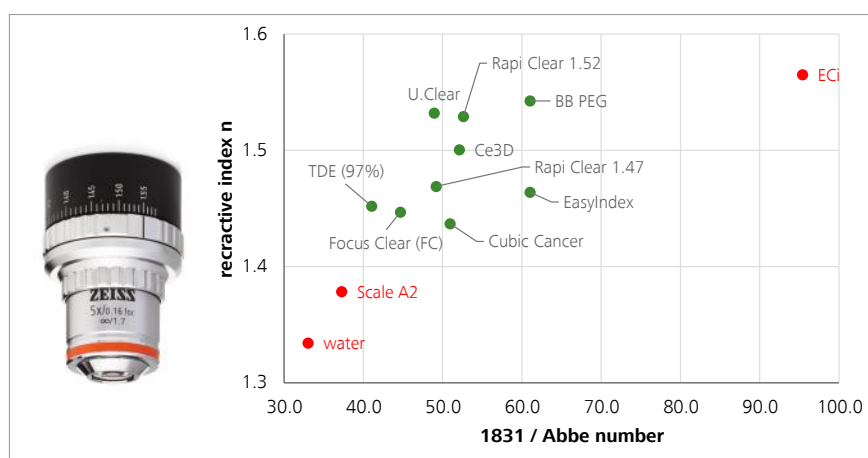


Figure 9 The design of the detection objective 5x/0.16 foc achieves minimal wavelength-dependent focus shifts (longitudinal chromatic aberrations) for a multitude of important imaging media (marked in green). However, extreme cases cannot be covered completely. For water (low dispersion) the objective selection for water should be used. For multi-color imaging in ethyl cinnamate appropriate image acquisition strategies or post processing channel alignment to compensate for chromatic effects is recommended.

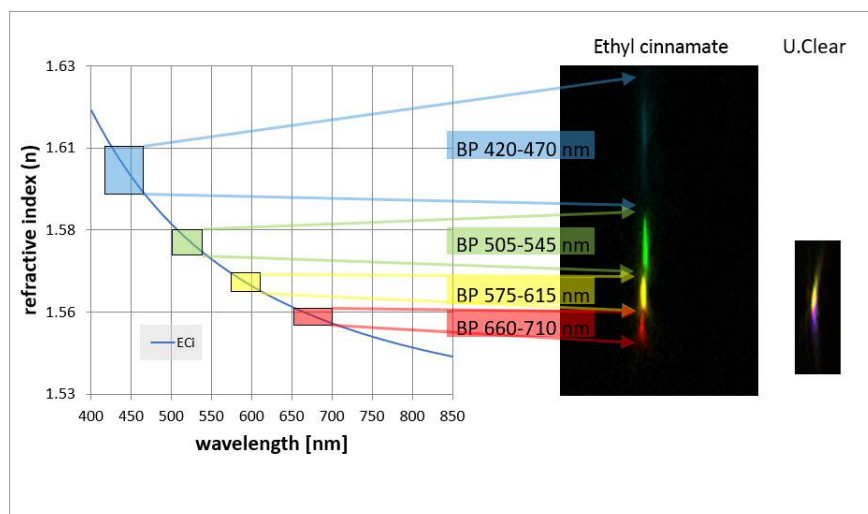


Figure 10 The strong dispersion of ethyl cinnamate induces a focal shift in the PSFs between the four wavelength channels. Furthermore, each channel shows a broadened extension along the optical (z) axis. This is most prominent for short wavelengths, where dispersion is strongest. The examples are given for the Clr Plan-NEOFLUAR 20 \times /1.0 $n_d=1.53$, which was designed for U.Clear and shows excellent color correction for this and similar imaging media (see the small PSF on the right).

However, there is imaging media for which such a compromise is not easily achieved. For multichannel experiments we then recommend software solutions that shift or align the different channels with respect to each other.

It is worth mentioning that not only shifts between different wavelength channels can occur, but also broadening of the point spread function for each channel may occur. This effect generally increases with dispersion mismatch and channel width (Figure 10).

Therefore, objective lenses perform best with the imaging media they were designed for. If experiments require using other imaging media, chromatic effects must be taken care of. Choosing narrow band pass filters might be one option, software corrections like channel alignment may be another.

Conclusion

Refractive index mismatches and aberrations influence image quality in LSM. Since these effects are strongly dependent on the optical and spectral properties of the specific imaging immersion medium in use, the recent trend of diversification and development of an increasing range of methods for optical clearing of tissue for imaging requires addressing them in microscope system design.

The newly designed optics of ZEISS Lightsheet 7 allow to flexibly tune the system to a whole range of imaging media and optical clearing agents. Focus rings (and correction collars for higher magnification objectives) together with special sample chambers allow to adapt the microscope to differences of the imaging media in use. To achieve best image quality, it is important to

know the refractive index and optical properties of the used medium and to then set optical and system parameters correctly. ZEN imaging software can help users setting up parameters for best image quality.

Appendix

As described above, the effect of a refractive index mismatch in the sample chamber results in a focus shift for the detection and illumination objectives and thereby in an increase of the thickness of the illumination light sheet.

In this appendix we provide some useful relations and formulas. In order to simplify our derivation, we limit the discussion to one objective only. All the following explanations apply to illumination and detection equally. On the left side of Figure 11, we show an objective-chamber combination made for a specific RI. Hence the sample chamber is filled with the correct medium (refractive index n_0) that the system is designed for and the focus lies in the middle of the chamber (chamber width $2L_0$). In a sample chamber filled with air ($n_1=1$) the focus of the illumination objective would be closer to the objective as indicated by the shorter, unrefracted cone. The radius of the light cone/light sheet at the entrance of the sample chamber is r_0 in both cases. If the chamber was instead filled with a medium of refractive index higher than e.g. water ($n_x > n_0$, right side of Figure 11) a focus shift away from the objective would be the result, but still the radius of the light cone/light sheet at the entrance of the sample chamber would be r_0 .

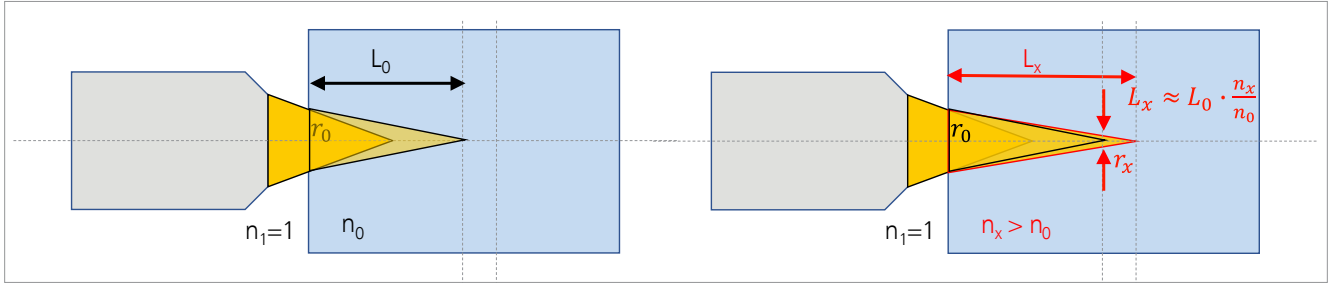


Figure 11 Focus shift occurs in an objective-chamber combination that is designed for one imaging medium (refractive index n_0) and used with another medium (n_x)

When entering the chamber, the illumination light undergoes refraction. The following equations incorporate the law of refraction for both situations shown in the figure. The numerical aperture (NA) is preserved.

$$NA = n_1 \cdot \sin(\alpha_1) = n_0 \cdot \sin(\alpha_0)$$

$$NA = n_1 \cdot \sin(\alpha_1) = n_x \cdot \sin(\alpha_x)$$

Taking into account that the radius of the light cone/light sheet at the entrance of the sample chamber is independent of the medium inside

$$\tan(\alpha_0) = \frac{r_0}{L_0}$$

$$\tan(\alpha_x) = \frac{r_0}{L_x}$$

we can easily find the position of the focal plane (beam waist). The first line of the below formula shows the exact expression and the second is an approximation for small angles that further simplifies the equation by using the law of refraction.

$$L_x = L_0 \cdot \frac{\tan(\alpha_0)}{\tan(\alpha_x)}$$

$$L_x \cong L_0 \cdot \frac{\sin(\alpha_0)}{\sin(\alpha_x)} = L_0 \cdot \frac{n_x}{n_0}$$

The small angle approximation results in errors $< 10\%$ for $NA < 0.5$ and $|n_0 - n_x| < 0.2$ and hence can be applied for the illumination in ZEISS Lightsheet 7 with its illumination optics of $NA = 0.1$ and 0.2 respectively. For detection optics with $NA \geq 0.5$ the exact formula is required.

This difference between tangent and sine describes the focal spread for different parts of the light cone depending on their respective angles with the optical axis. This optical aberration is called *spherical aberration*.

We can now derive the increased width r_x of the light sheet due to index mismatch. In the right sketch in Figure 11, a comparison of the black and the red triangle is shown:

$$\text{red: } r_x = (L_0 - L_x) \cdot \tan(\alpha_x)$$

$$\text{black: } r_0 = L_0 \cdot (\tan(\alpha_x) - \tan(\alpha_0))$$

For small angles (see above) the tangent can be approximated by the sine function, resulting in:

$$r_x \approx L_0 \cdot (\sin(\alpha_x) - \sin(\alpha_0)) = L_0 \cdot NA \cdot \left(\frac{1}{n_x} - \frac{1}{n_0} \right)$$

The analysis above is based on geometrical optics. This is appropriate in order to compute focal shift and increase in width of the light sheet. Nevertheless, even in the “design” case the width of the light sheet or any beam waist of light will not be zero but limited by optical diffraction. If we assume a finite value given by the wavelength of light λ it follows from the optic’s numerical aperture NA:

$$r_0 = 0.51 \frac{\lambda}{NA}$$

The nominal radius r_0 can be in the order of a few microns and a refractive index shift can result in a width of a few hundred microns.

Cover images:

Top left:

Sample courtesy of U. Roostalu, Gubra, Denmark.

Top right:

Sample courtesy of E. Diel, D. Richardson, Harvard University, Cambridge, USA.

Bottom left:

Sample courtesy of J. Groom, B. Duckworth, The Walter and Eliza Hall Institute of Medical Research, Parkville, Australia.

Bottom right:

Sample courtesy of P.-L. Ruffault, C. Birchmeier, Laboratory of Developmental Biology / Signal Transduction; A. Spörbert, M. Richter, Advanced Light Microscopy; M. Delbrück Center for Molecular Medicine, Berlin, Germany

References:

- [1] A more detailed explanation of the expressions can be found in the appendix.
- [2] Ueda, H. R. et al. *Nature Reviews Neuroscience* 1–19 (2019).
- [3] Masselink, W. et al. *Development* 146 (2019).
- [4] Yu, T. et al. *J. Biophotonics* 11 (2017).
- [5] Matryba, P. et al. *Laser & Photonics Reviews* 13 (2019).
- [6] U.Clear, Ce3D, Cubic Cancer and RapiClear® have substantially high refractive indices than e. g. ScaleView ($n=1.38$) and water ($n=1.33$)
- [7] NA is the *numerical aperture* of the illumination objectives. For details see appendix.
- [8] both are two consequences of the same optical effect
- [9] The higher magnification objectives have smaller working distances and – due to their usually high NA – work over a smaller range of refractive indices only. Both aspects reduce the focus shift.



Carl Zeiss Microscopy GmbH

07745 Jena, Germany

microscopy@zeiss.com

www.zeiss.com/lightsheet